

Synchrotron radiation induced gas desorption from a Prototype Large Hadron Collider beam screen at cryogenic temperatures

R. Calder, O. Gröbner,^{a)} and A. G. Mathewson
CERN, Geneva, Switzerland

V. V. Anashin, A. Dranichnikov, and O. B. Malyshev
Budker Institute of Nuclear Physics, Novosibirsk, Russia

(Received 20 November 1995; accepted 9 March 1996)

The performance of the vacuum system of the Large Hadron Collider will depend critically on the synchrotron radiation induced gas desorption and on the readsorption of molecules on the cold surfaces. The present design of the system is based on a so-called *beam screen* inserted in the 1.9 K cold bore of the magnets. Gas molecules desorbed will therefore readsorb on the beam screen which is held at a temperature between 5 and 20 K. Pumping slots in the beam screen enable some of the desorbed gas to be pumped onto the 1.9 K surface of the cold bore. © 1996 American Vacuum Society.

I. INTRODUCTION

In the present design of the Large Hadron Collider (LHC),¹ the beam screen consists of a 1 mm thick, square section (outer dimensions 38 mm×38 mm) stainless steel tube, with a 50 μm layer of Cu covering the whole of the inside surface. The beam screen will operate at a temperature of between 5 and 20 K.

The Cu coated beam screen will be inserted in the 1.9 K cold bore tube of the superconducting magnet and it is this Cu surface which will be subjected to bombardment by the 43.8 eV critical energy synchrotron radiation from the 7 TeV protons with the subsequent photon induced gas desorption. (Note: $T=10^{12}$.) Pumping of the system will rely entirely on cryosorption—partly on the cold surfaces of the beam screen and partly through pumping slots in the screen on the surface of the magnet cold bore.

In this article, we report on the measurements of the synchrotron radiation induced gas desorption from two prototype beam screens at 77 K and at a temperature between 4.2 and 10 K. We used synchrotron radiation with a critical energy of 50 eV from the VEPP-2M storage ring at the Budker Institute of Nuclear Physics in Novosibirsk, Russia.

II. BEAM SCREEN PREPARATION

A schematic cross-section of the proposed beam screen for LHC is shown in Fig. 1. The prototype beam screens used in this experiment each consisted of a 1 m long square section 304L stainless steel tube (38 mm×38 mm) with a strip of Cu 0.2 mm thick and 18 mm wide bonded to the inside of each flat side. The bonding was carried out by a skive inlay process² which essentially entails machining a fresh stainless surface before roll bonding the Cu onto it. In the process the resulting Cu/stainless steel sandwich was reduced in thickness to 1 mm. Two cooling pipes were soft soldered on to the outer surface.

Along the length of the beam screen were four rows of pumping slots 10 mm×1 mm, separated longitudinally by 5 mm and covering ~2% of the internal surface.

The complete beam screen was cleaned by degreasing in an alkaline detergent and then acid etched in a mixture of H₂SO₄, HNO₃ and HCl (only the Cu was attacked by the acid solution) followed by passivation of the Cu in CrO₃ (chromic acid). After rinsing in demineralized water, the beam screens were dried in a jet of N₂. The beam screens were transported to Novosibirsk in a sealed plastic bag filled with dry N₂.

III. EXPERIMENT

A. Beam line and cryogenic system

Desorption yields were measured on a dedicated synchrotron radiation beam line on the VEPP-2M electron-positron storage ring. This facility has been described fully in previous publications^{3,4} but for completeness, and since some modifications had to be made, a brief description of the apparatus will be given here.

Two beam lines—one for high intensity photon irradiation and one for low intensity—were originally constructed to measure photon induced gas desorption yields at room temperature and 4.2 K. These operated at a critical energy of 284 eV to provide input data for the design of the cold vacuum system of the 20 TeV Superconducting Super Collider (SSC). On the high intensity beam line, closer to the storage ring, a cryostat had been installed which enabled measurements to be made at 4.2 K.

The nominal energy of the VEPP-2M storage ring is around 500 MeV but to reproduce the low critical energy of the LHC it was run at an energy of 300 MeV which corresponds to a critical energy of 50 eV, close to the 43.8 eV of the LHC. At this energy the maximum beam current is about 300 mA. The linear photon flux incident on the test chamber is 1.57×10^{14} photons s⁻¹ m⁻¹ mA⁻¹, which is approximately 12% lower than for LHC with 1.78×10^{14} photons s⁻¹ m⁻¹ mA⁻¹. In practice, at 300 MeV the beam

^{a)}Electronic mail: oswald.groebner@cern.ch

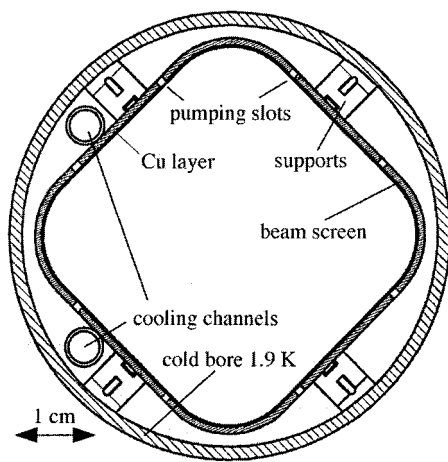


FIG. 1. A schematic diagram of the dipole magnet cold bore with the square beam screen containing pumping slots and two cooling channels to maintain the screen between 5 and 20 K.

lifetime was only some minutes and by reinjecting every few minutes the average beam current was kept above 200 mA. The synchrotron radiation was incident on one corner of the beam screen at a glancing angle of 10 mrad and illuminated almost the complete 1 m length. Total doses of up to 1×10^{22} photons m^{-1} could be accumulated over a period of about seven days. During the last part of this experiment (run No. 4), the critical energy was increased to 284 eV, the design value of the SSC.

A schematic view of the experimental setup is shown in Fig. 2. In the LHC, the beam screen will run at a temperature between 5 and 20 K and will be inserted in the magnet cold bore which will be at a temperature of 1.9 K. Thus the cryostat shown in Fig. 2 was modified to be able to cool the beam screen independently, using either liquid N_2 at 77 K or

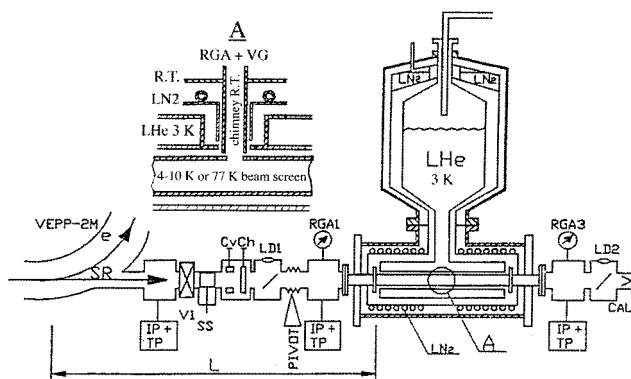


FIG. 2. The experimental setup for the cold beam screen experiment. V1—vacuum valve; Cv, Ch—vertical and horizontal collimators; SS—safety shutter; LD1, LD2—luminescent screens; VG—ionization gauge; RGA—residual gas analyzer; IP+TP—combination ion and Ti sublimation pump; L=1.75 m. A calorimeter is mounted at the end of the line. The inset (A) shows a schematic view of the pressure measuring arrangement between the test chamber with the 3 K cold bore and the beam screen which could be adjusted to temperatures between 293 and 10 K. Also shown is the arrangement of the room temperature pressure gauges and the chimney at approximately room temperature leading to the cold test volume.

gaseous He evaporated from a liquid He bath from which the flow was regulated to maintain a constant temperature of 10 K on the outlet of the beam screen cooling circuit. In turn, the beam screen was surrounded by the cryostat which was maintained throughout the experiment at a temperature below 3 K.

Of the gases desorbed by the synchrotron radiation, H_2 , CH_4 , CO , and CO_2 , only H_2 has a significant saturated vapor pressure in the range 4.2–10 K ($>10^{-6}$ Torr). This H_2 has to be pumped by the cold bore surrounding the beam screen. Thus the cold bore temperature in the experiment should be such that the saturated vapor pressure of the condensed H_2 is less than about 10^{-10} Torr. This implies that its temperature must be less than 3 K. Due to this fact it was not necessary to cool the cold bore to the LHC value of 1.9 K and longer experimental runs could be carried out for a given liquid He capacity.

B. Gas density and molecular desorption yield

In the experiment, by necessity, all vacuum gauges and the gas analyzer were at room temperature. In an earlier experiment,⁵ the chimney connecting these instruments to the cold desorbing zone was at 77 K. It was reasoned that with this chimney at a higher temperature—but still compatible with heat input to the cold zone—there would be an improved chance of being able to detect all of the desorbed gases, including CO_2 . Thus the cryostat was modified to have the temperature of the chimney close to 293 K and thus avoid any sticking of the molecules once they enter it. The insert in Fig. 2 shows schematically the details of the position of this room temperature chimney with respect to the measuring instruments, the thermal screen at 77 K, the cold bore at <3 K, and the beam screen.

The gas density n and the pressure P inside the beam screen at the temperature T was calculated from the room temperature measurements (subscript RT) using the expressions

$$n = n_{RT} \sqrt{\frac{T_{RT}}{T}}; \quad P = P_{RT} \sqrt{\frac{T}{T_{RT}}},$$

respectively.

The contribution of the background pressure (P_0) was measured at many instances throughout the series of experiments by stopping temporarily the photon beam to the test system (as shown by the lower set of measured points in Fig. 4). For the evaluation of the molecular desorption yield η the background values were subtracted to arrive at the net increase in gas density inside the beam screen

$$\Delta n = \frac{(P - P_0)_{RT}}{k \sqrt{TT_{RT}}}$$

and finally

$$\eta = \frac{\Delta n S}{\Gamma}.$$

Here k is the Boltzmann constant, S represents the linear pumping speed and $\bar{\Gamma}$ is the linear photon flux in the test chamber as provided by the VEPP-2M storage ring. The pumping by the surface of the beam screen and by the pumping slots in the beam screen is proportional to the mean molecular velocity v

$$v = \sqrt{\frac{8kT}{\pi m}} \approx 145 \sqrt{\frac{T}{M}}, \quad (\text{m s}^{-1}),$$

where m is the mass of the molecules and M their molecular weight.

For a molecular sticking probability of s on the screen and complete adsorption in the pumping slots the resulting pumping speed for unit length of beam screen (surface area F) with pumping slots (area f, F) is

$$S = \frac{1}{4}vF(s+f).$$

Combining the above expressions gives for the molecular desorption yield

$$\eta = \sqrt{\frac{1}{2\pi}} \frac{F(s+f)}{\bar{\Gamma}} \frac{(P-P_0)_{\text{RT}}}{\sqrt{mkT_{\text{RT}}}}.$$

It is interesting to note that this result for η becomes independent of the temperature T of the cold system.

Entering the numerical constants, and using units of Pa for the pressure gives

$$\eta \approx 2.64$$

$$\times 10^{24} \frac{F(s+f)}{\bar{\Gamma}} \frac{(P-P_0)_{\text{RT}}}{\sqrt{MT_{\text{RT}}}} \quad (\text{molecules per photon}).$$

For the evaluation of the data from the different experimental runs, two extreme situations occur: when the screen is at a sufficiently high temperature or saturated with gas such that it does not absorb, $s=0$; when the screen is at low temperature and not saturated, $0 < s < 1$. The latter situation is not useful without an independent measure of s . In this work we evaluate η in conditions where it may be assumed that $s \rightarrow 0$ and the only pumping is a well defined value provided by the area of the pumping slots.

IV. PHOTON INDUCED DESORPTION

A. Measurements at 77 K

The desorption yield measured with the beam screen at a temperature of 77 K is shown in Fig. 3 as a function of the photon dose. Compared with equivalent room temperature measurements, the data for H_2 are in good agreement.⁶

For this experiment the molecular desorption yield η was calculated from the partial pressure increase making the assumption that the beam screen surface had a vanishing net pumping effect, i.e., that its surface coverage of adsorbed molecules had reached an equilibrium with the gas phase. Therefore, the only contribution to the pumping of the system was that given by the conductance of the pumping slots in the beam screen leading to adsorption on the 3 K surface

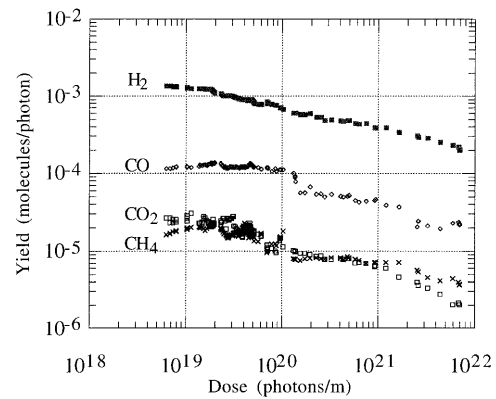


FIG. 3. Desorption yields for the dominant gas species as a function of the photon dose for a beam screen temperature of 77 K.

of the cold bore. This assumption should be well satisfied for H_2 , but may not be a good approximation for the other gases.

Indeed, when comparing with room temperature results, CO and CO_2 show a significantly lower desorption yield.⁷ Whether this effect is real, i.e., the desorption of CO and CO_2 molecules is reduced at cryogenic temperature—or can be attributed simply to a non-zero sticking probability on the 77 K beam screen—is uncertain. Further studies are required to confirm this observation.

B. Measurements at 4.2–10 K

As a sequel to the first measurements at 77 K, a new beam screen was installed and exposed to synchrotron radiation at a temperature which could have ranged, along its length, between the limits of 4.2 and 10 K (runs No. 1 and No. 2). During runs No. 3 and No. 4, the temperature of the beam screen was again raised to 77 K and in addition, for run No. 4 also the critical energy of the photon spectrum was increased to 284 eV (the value of previous measurements for the SSC).

Throughout the experiment, individual measurements were performed by taking the differences of the pressure readings obtained with and without photon irradiation. This procedure was adopted because the pressure increases were small compared to the base pressure and because any increase of the base pressure due to a contribution from the vapor pressure of adsorbed gas molecules would have been readily detected. The data presented in Fig. 4 illustrate the increase of the dynamic pressure, while the constant level of the *photon-off* pressure suggests that the vapor pressure remained below the instrumental background of approximately 4×10^{-10} Torr throughout the four individual runs.

The molecular desorption yield calculated for H_2 is shown in Fig. 5 as a function of the photon dose.

These values have been derived from the quasi steady state values in Fig. 4 for which it was assumed that the screen surface had reached saturation and therefore the net pumping speed was given by the known conductance of the slots in the beam screen. Inspection of the data in Fig. 5 shows a slow cleaning-up of the beam screen throughout the runs Nos. 1–4. It should be noted that the desorption yield at 77 K during run No. 3 shows no increase with respect to the

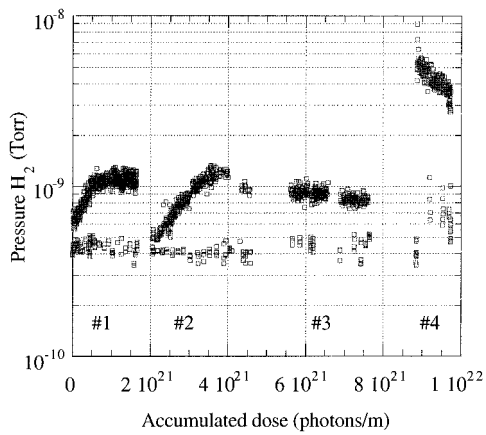


FIG. 4. Summary results for the room temperature hydrogen pressure during photon exposure between 4.2 and 10 K (No. 1 and No. 2) and at 77 K (No. 3 and No. 4) showing the difference between photons on and off. The lower points correspond to photons off. For run No. 4, the critical energy of the synchrotron radiation spectrum was increased from 50 to 284 eV. Here the H_2 pressure increase, as measured at room temperature, has been normalized to a beam current of 300 mA in the VEPP-2M storage ring.

10 K measurements while the increased yield during run No. 4 is consistent with a linear dependence on the critical photon energy.⁸

The first two runs No. 1 and No. 2 give a very clear illustration of the gradual increase of the dynamic pressure due to the buildup of adsorbed gas on the beam screen and the saturation level imposed by the constant pumping speed through the slots in the beam screen. Between run No. 1 and run No. 2 the beam screen was warmed up to 77 K while maintaining the surrounding cold bore at its constant temperature of 3 K. Figure 6 shows the two successive runs.

During the temporary warm-up to 77 K between run No. 1 and run No. 2 accumulated H_2 is desorbed from the screen and is permanently adsorbed on the outer 3 K surface. Therefore, run No. 2 is a repetition of run No. 1 with the only exception that the surface has been cleaned to a small degree by the additional photon exposure (e.g., see Fig. 3 for the expected reduction of the molecular yield).

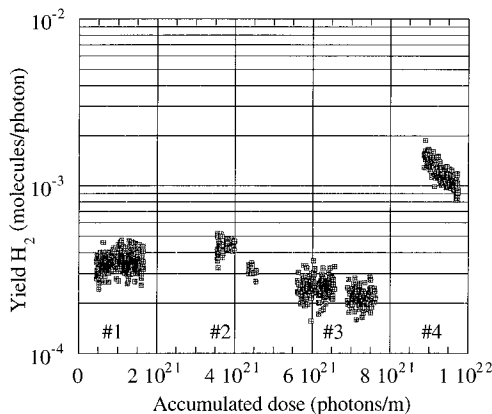


FIG. 5. Summary results of the molecular desorption yield for H_2 during the four exposures to synchrotron radiation (see Fig. 4 for comments).

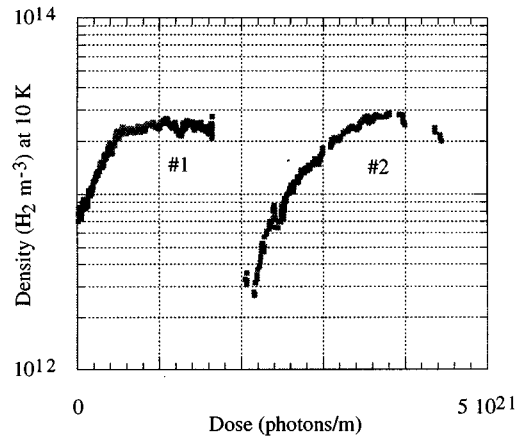


FIG. 6. Evolution of the molecular density of H_2 during the photon exposure. The temperature of the beam screen is ≤ 10 K. The beam screen was warmed up to 77 K between the two runs. After subtracting a constant background (equivalent to 4×10^{-10} Torr at room temperature; see Fig. 4) the H_2 density has been renormalized to a VEPP-2M beam current of 60 mA to give a photon flux equivalent to 53 mA in LHC.

V. DYNAMIC MODEL FOR H_2

The dynamic behavior of hydrogen observed in this experiment may be described very closely by assuming a linear model for the interaction between the volume density, $n(\text{m}^{-3})$, and the surface density, $\theta(\text{m}^{-2})$, of adsorbed molecules. Apart from the replacement of ion induced desorption by photon stimulated desorption, this model is very similar to the analysis of the dynamic pressure in the ISR vacuum system.⁹ The volume and the surface gas interact according to the following set of linear equations

$$V \frac{dn}{dt} = q - an + b\theta$$

and

$$F \frac{d\theta}{dt} = cn - b\theta.$$

Here, V is the volume and F is the net wall area per unit length of the vacuum system excluding the area of the pumping holes. The parameters a , b , c and q are assumed to be constant.

q represents a constant source of gas, here in particular the photon induced desorption rate determined by the product of the desorption yield η and of the photon flux $\dot{\Gamma}$ hence $q = \eta \dot{\Gamma}$ ($\text{molecules s}^{-1} \text{m}^{-1}$).

a describes the total pumping on the surface of the wall and through the area of the holes in the beam screen. It can be expressed as

$$a = \frac{1}{4} v F (s + f), \quad (\text{m}^2 \text{s}^{-1}),$$

where v is the average molecular velocity, s the sticking probability of the molecules on the beam screen and f is the fraction of the total surface of the beam screen with pumping holes, $f \ll 1$.

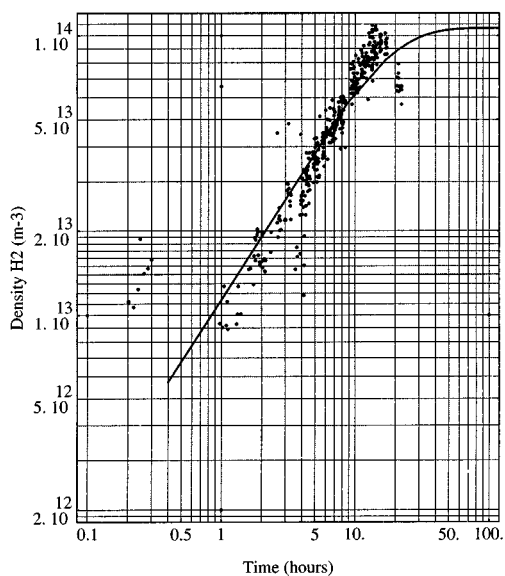


FIG. 7. Comparison of the H₂ data from run No. 2 with the dynamic model of desorption and recycling of H₂ molecules. The specific parameters which have been used are summarized in Table I.

b represents the gas source originating from the adsorbed surface phase θ by thermal and by photon induced desorption.

The thermal contribution¹⁰ may be expressed as the molecular vibration frequency $\nu_0 = 10^{13} \text{ s}^{-1}$ multiplied with a Boltzmann factor $e^{-E/kT}$ containing the activation energy *E*.

The photon induced desorption from the adsorbed phase does not represent a source of new gas molecules but simply recycles molecules adsorbed on the inner side of the beam screen. It is expressed as $\kappa\dot{\Gamma}$, where *k* is the recycling cross section in m² per photon, thus

$$b = F\nu_0 e^{-E/kT} + \kappa\dot{\Gamma}, \quad (\text{m s}^{-1}).$$

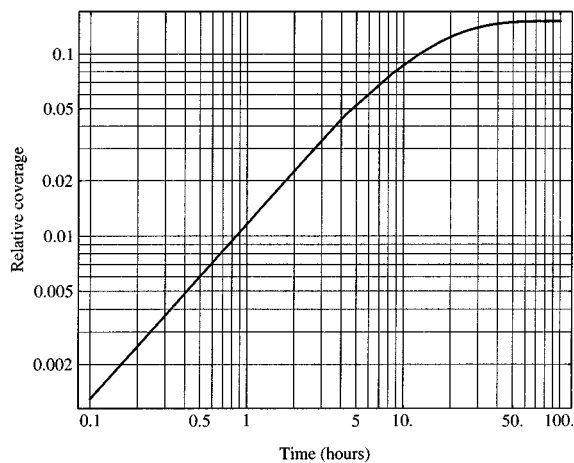


FIG. 8. Surface density of H₂ molecules normalized to a monolayer coverage as a function of time.

TABLE I. Parameters for the dynamic model of H₂.

Desorption yield	η	5×10^{-4} molecules/photon
Screen temperature	<i>T</i>	10 K (maximum)
Linear photon flux (200 mA)	$\dot{\Gamma}$	3.14×10^{16} photons/s ⁻¹ m ⁻¹
Sticking probability	<i>s</i>	0.6
Fraction of slots	<i>f</i>	1.28%
Monolayer capacity		3×10^{19} molecules/m ²
Recycling cross section	κ	5×10^{-21} m ²
Activation energy	<i>E</i>	800 cal/mol (0.035 eV/molecule)
Specific surface area	<i>F</i>	0.14 m
Specific volume	<i>V</i>	1.3×10^{-3} m ²

c is the rate of adsorption of gas molecules on the surface of the beam screen only. This expression contains the sticking probability of the molecules, *s*,

$$c = \frac{1}{4}v_s F, \quad (\text{m}^2 \text{ s}^{-1}).$$

This model contains a small number of free parameters and implies a linear adsorption isotherm, i.e., Henry's law applied to a limited range of interest:

$$\theta = \frac{c}{b} n = \frac{1/4v_s F}{F\nu_0 e^{-E/kT} + \kappa\dot{\Gamma}} n.$$

Here $\theta(n)$ depends on the recycling cross section as well as on the photon flux. Therefore, the isotherm and the equilibrium surface coverage for a given volume gas density will depend on the specific conditions (i.e., on the beam current) during the experiment which effectively reduce the sojourn time of the physisorbed molecules.

As is shown for run No. 2 in Fig. 7, the results can indeed be described in a fairly satisfactory manner by this simple model by adapting the free parameters summarized in Table I.

Parameters in Table I shown in bold face have been adapted to obtain the curves in Figs. 7 and 9. The fraction of

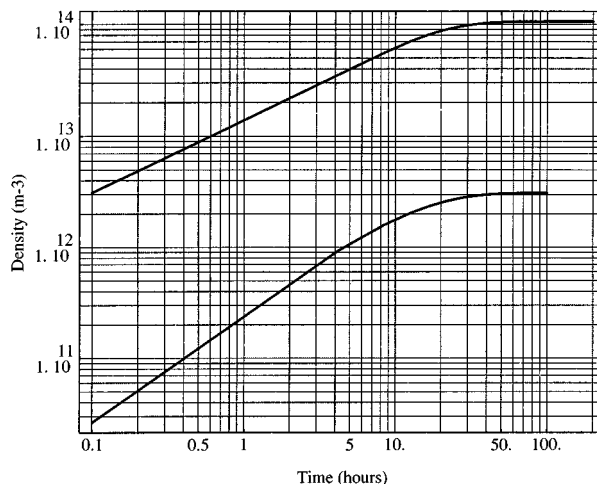


FIG. 9. Upper curve shows the gas density with photon exposure and lower curve shows the gas density without photons.

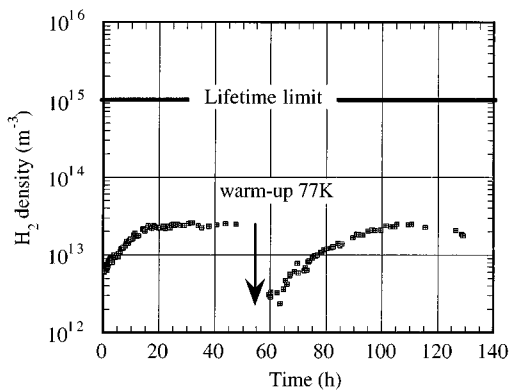


FIG. 10. Dynamic H_2 pressure in LHC with an initial beam current of 53 mA derived from the results of the first two runs.

slots has been corrected for the Clausing factor due to the thickness of the beam screen.

The model provides in addition to the volume density also the surface density of gas, θ , shown in Fig. 8. There it can be seen that the final coverage obtained remains well below a monolayer.

As a further result, Fig. 9 gives the calculated volume densities as a function of time with photons on and photons off. The lower curve (photons off) corresponds to the equivalent measurements in Fig. 4 and gives the vapor pressure of the adsorbed gas. Considering that the lowest detectable pressure rise in the system corresponds to a density of approximately 8×10^{12} molecules m^{-3} , it is not surprising that the calculated increase in vapor pressure could not be observed during the runs.

VI. LHC PERFORMANCE

The test system and the beam screen used for these measurements very closely reproduce the conditions in LHC. At 200 mA in VEPP-2M, the linear photon flux in the test system is only about a factor of 3 lower than that in the LHC at 7 TeV and with the nominal beam current of 536 mA. To obtain an estimate of the vacuum performance during LHC operation, it was therefore sufficient to scale with the linear photon flux since both the close rate and H_2 density in the beam screen depend linearly on the photon flux. The scaling of runs No. 1 and No. 2 to LHC conditions with an initial beam current of 53 mA but without modifying the area of pumping slots is shown in Fig. 10. Here the dose scale has been converted to running time in hours to illustrate the short time necessary to reach the stationary density due to the density limiting effect of the pumping holes. Without holes, the density would continue to rise and would exceed the maximum tolerable level within a few days of operation.

The lifetime limit of 10^{15} molecules m^{-3} for H_2 is determined for LHC by the tolerable rate of particle loss from the beam and corresponds to a beam lifetime of approximately 100 h. So far only H_2 has been taken into account. In a real vacuum system, the contribution of all other gas species has to be added in proportion of their respective cross sections

and thus the apparently comfortable vacuum performance shown in Fig. 10 may not be achieved. For this reason, and in order to meet the vacuum requirements, with the 10 times larger nominal beam current (536 mA), the LHC beam screen will need a substantial amount of *in situ* cleaning by synchrotron radiation in the same way as for electron machines.

Important for the design of the LHC vacuum system will be the total amount of H_2 desorbed. This quantity may be estimated from an extrapolation of the H_2 data in Fig. 3 where it can be seen that the yield as a function of photon dose may be approximated by

$$\eta = \eta_0 \left(\frac{D}{D_0} \right)^{-1/3},$$

with $\eta_0 = 10^{-3}$ molecules/photon and $D_0 = 2 \times 10^{19}$ photons m^{-1} . The accumulated photon dose in LHC during the first year will be of the order of 10^{23} photons m^{-1} and, thus, one can estimate that the equivalent of 2.6 monolayers of H_2 will be desorbed from the beam screen. During the second year—at the full nominal beam current—the equivalent of 10.5 monolayers will be desorbed. This total quantity of gas should not pose a problem within the present design of the LHC vacuum system since the molecules can diffuse through the pumping holes and be adsorbed on the 1.9 K cold bore with a negligible vapor pressure.

ACKNOWLEDGMENTS

The authors gratefully acknowledge the numerous contributions to this work by Dr. W. Turner who initiated the first phase of these studies in the context of the SSC vacuum system design and thus laid the foundations for the continuation of this program for the LHC. They would also like to thank the operations crew of the VEPP-2M machine for providing the special running conditions for this experiment.

¹The LHC Study Group, The Large Hadron Collider Accelerator Project, CERN/AC/93-03 (LHC), 1993.

²Technical Materials, Inc., 5 Wellington Road, Lincoln, RI, USA.

³V. V. Anashin, O. B. Malyshev, V. N. Ossipov, I. L. Maslennikov, and W. C. Turner, *J. Vac. Sci. Technol. A* **12**, 2917 (1994).

⁴I. Maslennikov *et al.*, *Proceedings of the 1993 IEEE Particle Accelerator Conference, Washington, 17–20 May* (IEEE, New York, 1993), p. 3876.

⁵V. Anashin *et al.*, *Proceedings of the 4th European Particle Accelerator Conference, London, 27 June–1 July 1994*, edited by V. Suller and Ch. Petit-Jean-Genaz (World Scientific, London, 1994), p. 2506.

⁶C. L. Foester, C. Lanni, I. Maslennikov, and W. Turner, 41st National Symposium of the American Vacuum Society, Denver, CO, October 1994 (unpublished), VT-TuM3.

⁷J. Gómez-Goni, O. Gröbner, A. G. Mathewson, and A. Poncet, *Proceedings of the 3rd European Particle Accelerator Conference, Berlin, 24–28 March 1992*, edited by H. Henke, H. Homeyer, and Ch. Petit-Jean-Genaz (Edition Frontières, Paris, 1992), p. 1576.

⁸J. Gómez-Goni, O. Gröbner and A. G. Mathewson, *J. Vac. Sci. Technol. A* **12**, 1714 (1994).

⁹O. Gröbner, CERN/ISR/VA/76-25, 1976 (CERN Internal Report).

¹⁰P. Redhead *et al.*, *The Physical Basis of Ultrahigh Vacuum* (AIP, New York, 1993).